

# Theoretical analysis of the effects of guanine oxidative damage on the properties of B-DNA telomere fragments

Piotr Cysewski · Przemysław Czeleń

Received: 14 November 2006 / Accepted: 6 February 2007 / Published online: 6 March 2007  
© Springer-Verlag 2007

**Abstract** The molecular dynamics as well as *ab initio* MP2/6-31G(d=0.25) single point calculations were performed for native and oxidized B-DNA telomeric fragments. The structural, dynamic, energetic and electrostatic properties along with frontier orbitals distribution were described for the central triad consisting of three guanine molecules in its canonical or oxidized forms. Although the average structural parameters characterizing all of the studied telomere fragments are close each to other, the significant consequence on angular and displacement flexibilities are observed. Namely, the increase of mutual displacement of two successive base pairs along either axis and increase of the rotation of two bases of opposite strand are main dynamic consequences of presence of 8-oxo-guanine in the central triad of telomeric B-DNA. Besides, the significant increase of stacking energies in case of 8-oxo-guanine were found. Furthermore, the guanine pattern visible from the major groove may be described as donor-acceptor-acceptor formed by H<sub>8</sub>-N<sub>7</sub>-O<sub>6</sub> atoms, respectively. To the contrary the presence of 8-oxo-guanine changes the electrostatic properties of the major groove into acceptor-donor-acceptor

coming from O<sub>8</sub>-H<sub>7</sub>-O<sub>6</sub> atoms. This results in significant alteration of ESP characteristics. Finally, the molecular orbital properties are also significantly affected by oxidation of telomeric B-DNA fragments. All these factors contribute to decrease of binding of telomere proteins.

**Keywords** B-DNA · 8-oxo-guanine · GGG triad · Molecular modeling · Oxidative damage · Telomeres

## Introduction

Telomeres are important protein-DNA complexes capping the ends of linear chromosomes [1]. Such structures are supposed to protect the chromosome ends and prevent them from being recognized and processed as DNA double strand breaks [2]. Telomeres play a critical role in keeping genomic stability and their dysfunction results in telomere end fusions, apoptosis or senescence [3]. Mammalian telomeres contain several kilbases of double-stranded AGGGTT repeat units providing docking sites for two related DNA binding proteins, TRF1 [4] and TRF2 [5]. Telomeres are regarded as “mitotic clock” due to their regular shortening with each cell division by about 20–200 base pairs in human somatic cells [6–8]. There was also observed significant increase of erosion and loss of telomeric DNA in human fibroblasts after mild oxidative stress-induced by hyperoxia, mitochondrial dysfunction, arsenic or UV irradiation [9, 10]. The mechanism of the enhanced telomere shortening rate as a result of damage of free oxygen radicals to the telomeric DNA was related to accumulation of single-stranded regions caused by lower repair of these terminal lesions compared to other regions [11]. Interestingly, the antioxidant treatment prevented telomere attrition. On the other hand, the telomeres formation is highly affected by oxidative lesion

**Electronic supplementary material** The online version of this article (doi:10.1007/s00894-007-0186-7) contains supplementary material, which is available to authorized users.

P. Cysewski · P. Czeleń  
Physical Chemistry Department, Collegium Medicum,  
Nicolaus Copernicus University,  
Kurpińskiego 5,  
85-950 Bydgoszcz, Poland

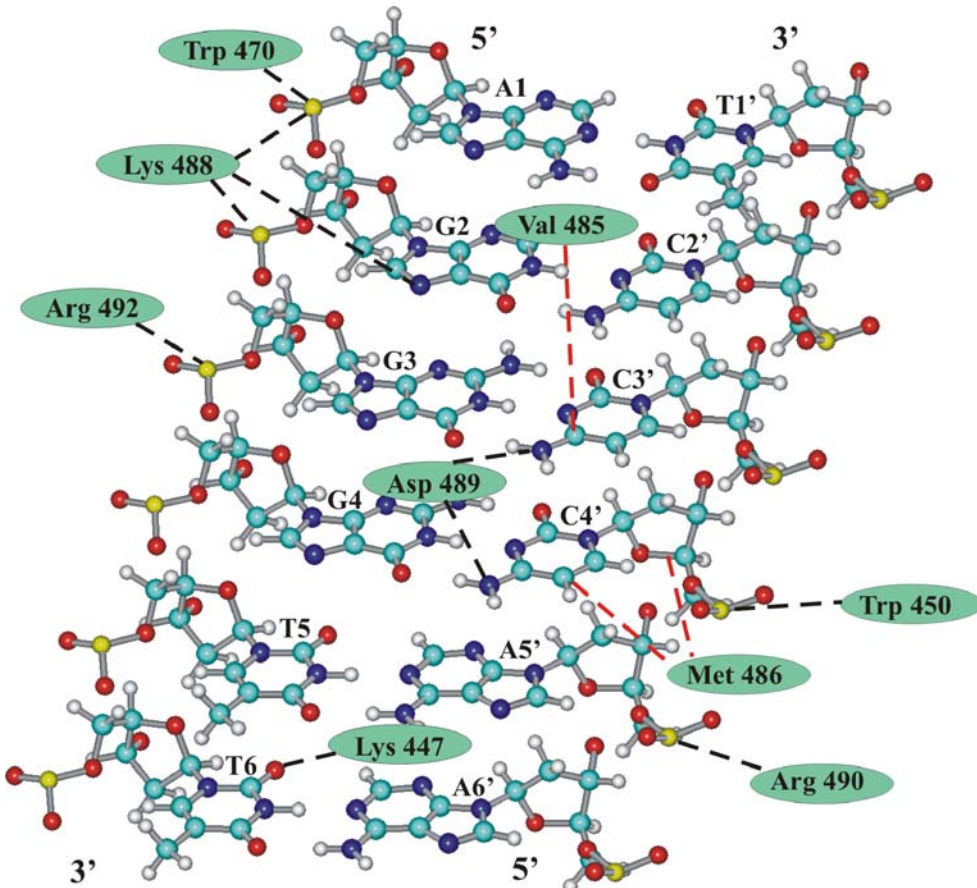
P. Cysewski (✉)  
Faculty of Chemical Technology and Engineering, General  
Chemistry Department, University of Technical and Agriculture,  
Semenyjna 3,  
85-326 Bydgoszcz, Poland  
e-mail: piotr.cysewski@cm.umk.pl

formation both in vivo and in vitro. For example [12] presence of single 8-oxo-guanine in telomeric DNA reduced the percentage of protein binding by factor equal to 50%, compared with standard non-damaged DNA. The presence of multiple 8-oxo-guanine lesions in GGG telomeric repeats, have more dramatic consequences and make the binding process nearly impossible. However, the consequences of DNA lesions in telomeric DNA on structure and function are not understood up till now. It is known that most abundant product of hydroxyl radical the modified guanine at C<sub>8</sub> position adopts 6,8-diketo form [13], which significantly differ in its donor-acceptor properties compared to native guanine. The alteration of interaction abilities of modified B-DNA major groove is of special importance since both TRF1 and TRF2 interact with the same A<sub>1</sub>G<sub>2</sub>G<sub>3</sub>G<sub>4</sub>T<sub>5</sub>T<sub>6</sub> binding site [14] by placing N-terminal arm strongly interacting with ribose-phosphate backbone on both sides of the major groove. The simplified description of TRF1 interactions is summarized in Fig. 1 [15]. These direct contacts of amino-acid side chains along with an extensive network of indirect water-mediated contacts orient the protein binding domain on such a way that recognition helix enters the DNA major groove making sequence-specific hydrogen bonds to the G-C base-pair triplet of the binding site. The protein DNA-binding domains dock onto

the DNA through direct interaction with the ribose phosphate backbone on both sides of the major groove and the N-terminal arm. In the major groove there are hydrophobic contacts of the valine and alanine methyl groups with the methyl group of thymine T<sub>6</sub>. The G<sub>2</sub> guanine is recognized by bifurcated hydrogen bond formed by lysine, which additionally interacts with two neighboring phosphate groups. The aspartic acid side chain makes two hydrogen bonds to two adjacent cytosines C<sub>3'</sub> and C<sub>4'</sub>. The methyl groups of methionine, valine and mentioned above aspartic acid form a hydrophobic cluster with C<sub>4'</sub> and C<sub>3'</sub> bases as well as with the backbone sugar of C<sub>4'</sub>. Although different amino acids are responsible for the TRF1 and TRF2 binding to DNA the mechanism is common for both proteins. For example Lys421 of TRF1 and Lys48 of TRF2 bind to G<sub>2</sub>, Arg425 of TRF2 and Arg492 of TRF2 recognizes G<sub>3</sub>. Thus, the central triad of telomeric fragment is one of the most significant patterns recognized by telomeric proteins (Fig. 1).

Thus, the GGG triad of telomeric B-DNA fragment seems to be crucial for specific recognition and binding of telomere protein. This study intends to analyze structural, dynamic, energetic, molecular orbital and electrostatic consequences of telomeric DNA oxidation in context of observed reduction of TRF1 and TRF2 binding affinities to modified telomeric B-DNA fragments.

**Fig. 1** The most probable mechanism of DNA telomeric fragments recognitions by TRF1 and TRF2 protein binding domains



## Methods

The initial structure of modeled B-DNA double strand consisting of 24 pairs of nucleic acid bases was prepared with the aid of 3DNA program [16]. Phosphate groups were neutralized by the adding of 46  $\text{Na}^+$  cations. The whole system was immersed in a water box with periodic boundary conditions. The TIP3P model for water molecules was applied. The AMBER forcefield supplemented by parameters for oxidized guanine were used [17]. The details about sequences of modeled DNA oligomers are presented in Table 1. For reducing the impact of initial conditions, the starting A structure coming directly from 3DNA program was used in preliminary molecular dynamics simulations. After stabilization of energies and RMS values during 200 ps run the actual molecular dynamics was performed. The A oligonucleotide obtained during this preliminary run was then used for preparation of other sequences described in Table 1. After modification of one, two or three guanine molecules the starting B, C and D oligomers were obtained. The molecular dynamics simulations were 1200 ps long and last 1000 ps were used for snapshots collection and data averaging in 10 ps interval. During all molecular dynamics calculations the 10 Å cutoff was applied. The AMBER 8.0 [18] program was used. Details of time evolution of structures A and B were presented in Fig. 2. Although data are available for the whole 24-mer only central telomeric fragments were analyzed in details. Each consisted of one of the following sequence:  $\text{G}_2\text{G}_3\text{G}_4$ ,  $\text{G}_2\text{X}_3\text{G}_4$ ,  $\text{G}_2\text{X}_3\text{X}_4$  and  $\text{X}_2\text{X}_3\text{X}_4$  for A, B, C and D oligomers, respectively. Symbol X denotes 8-oxo-guanine. The averaged parameters defining mutual orientations of nucleic acid bases were used for preparation of bi- or three molecular complexes. Their energetic, electrostatic and frontier orbital properties were then obtained based on MP2/6-31G(d=0.25) single point calculations. The utilization of a post-SCF framework is absolutely necessary especially in case of description of stacked complexes, what was previously demonstrated [19, 20], where further methodological details may be found. Briefly speaking, the MD calculations were used as the source of the intermolecular parameters, while actual geometries of bases were taken

**Table 1** The sequences of B-DNA oligomers used in MD simulations

Oligonucleotide	B-DNA sequence (5'→3')
<b>A</b>	CCGTACTT-A <sub>1</sub> <b>G<sub>2</sub>G<sub>3</sub>G<sub>4</sub>T<sub>5</sub>T<sub>6</sub></b> -AGGGTT-AACA
<b>B</b>	CCGTACTT-A <sub>1</sub> <b>G<sub>2</sub>X<sub>3</sub>G<sub>4</sub>T<sub>5</sub>T<sub>6</sub></b> -AGGGTT-AACA
<b>C</b>	CCGTACTT-A <sub>1</sub> <b>G<sub>2</sub>X<sub>3</sub>X<sub>4</sub>T<sub>5</sub>T<sub>6</sub></b> -AGGGTT-AACA
<b>D</b>	CCGTACTT-A <sub>1</sub> <b>X<sub>2</sub>X<sub>3</sub>X<sub>4</sub>T<sub>5</sub>T<sub>6</sub></b> -AGGGTT-AACA

The detailed structural, dynamic, energetic and electronic analysis was performed for central telomeric triad-fragments marked with bold letter, where X stands for 8-oxo-guanine.

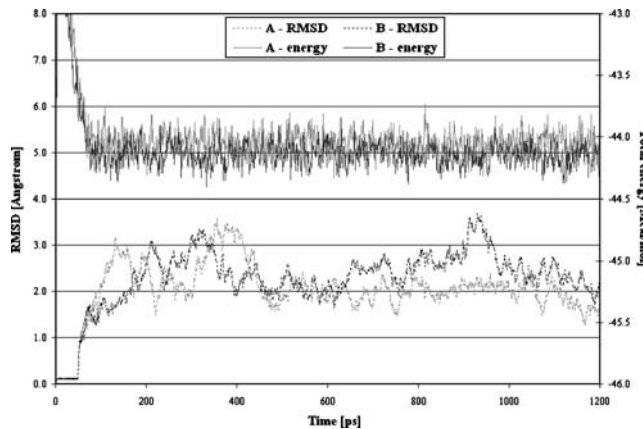


**Fig. 2** Characteristics of molecular dynamic simulations for telomeric fragments A and B. The period of last 1000 ps was used for averaging

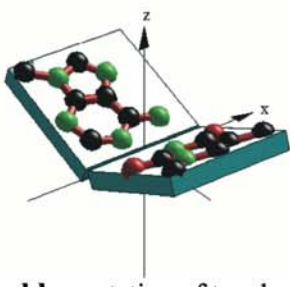
from subsequent optimization on MP2/6-31G(d=0.25) level. All structures analyzed on the *ab initio* level were generated in 3DNA program with non-standard monomers coming from subsequent /6-31G(d=0.25) optimization with  $C_s$  symmetry. The computation costs of MP2 calculations prevent from detailed studies of more complex telomeric fragments. All the *ab initio* calculations were performed with the aid of Gaussian03 package [21] and visualizations were prepared in GaussView program [22].

## Results and discussion

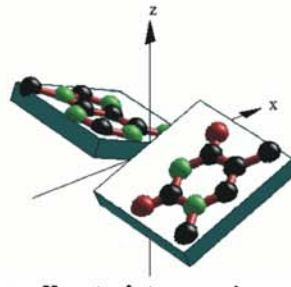
### Structural and dynamic consequences of guanine oxidation

Structural properties of DNA are defined by parameters describing mutual orientation of base pairs within one strand and two opposite strands of double helix [23]. Figure 3 summarizes definition of these parameters. To the first class belong so called shear, stretch, stagger, buckle, propeller, and opening. The second class comprises shift, slide, rise, tilt, roll, and twist. First three parameters of either class are expressed in Angstroms, while the last three are given in degrees. Half of these parameters as buckle, opening, propeller, shear, stretch, and stagger characterize mutual orientations of two bases of the opposite strands. The rest parameters declare intermolecular configuration within one strand. Thus, the first set may be used for description of hydrogen bonding, while the second one may be applied for analysis of stacking abilities. The molecular dynamics simulations provide detailed information, which may be used for structural characteristics of telomeric DNA fragments and the impact of oxidation on structural properties of GGG triad, its flexibility and structure may be analyzed in details. The flexibility is here defined as the time percentage, in which the values of parameters vary by certain amount from averaged ones. Such definition of what

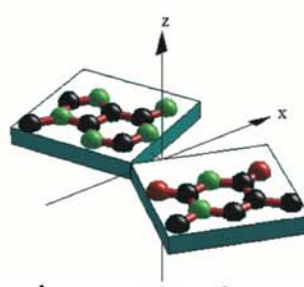
## angular parameters



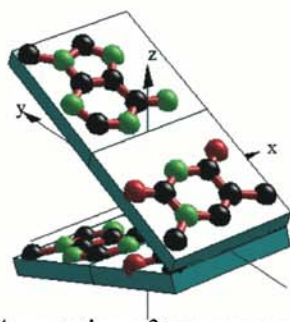
**buckle** - rotation of two bases of a pair about X axis



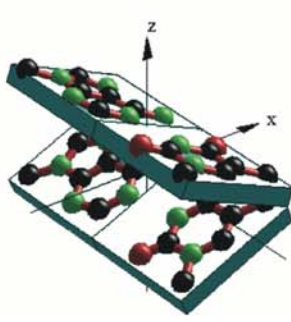
**propeller twist** - rotation of two bases of a pair about Y axis



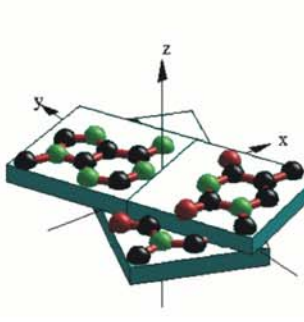
**opening** - rotation of two bases of a pair about Z axis



**tilt** - rotation of two successive base pairs about X axis

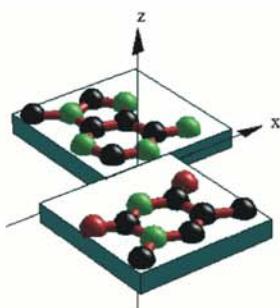


**roll** - rotation of two successive base pairs about Y axis

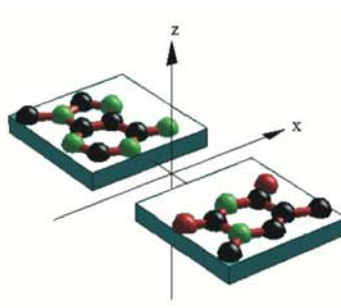


**twist** - rotation of two successive base pairs about Z axis

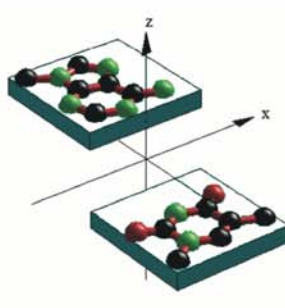
## displacement parameters



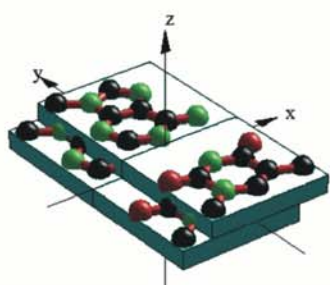
**shear** - mutual displacement of two bases of a pair along X axis



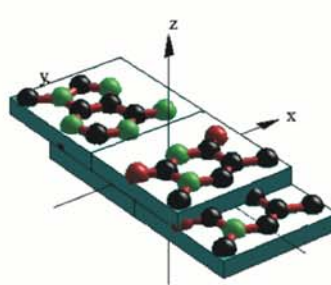
**stretch** - mutual displacement of two bases of a pair along Y axis



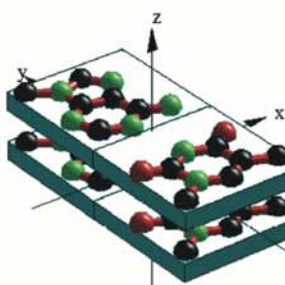
**stagger** - mutual displacement of two bases of a pair along Z axis



**shift** - mutual displacement of two successive base pairs along X axis



**slide** - mutual displacement of two successive base pairs along Y axis



**rise** - mutual displacement of two successive base pairs along Z axis

**Fig. 3** Parameters used in description of conformation of DNA double helix

lies outside the norm has an arbitrary character but it is consistent for all structures and is suitable for qualitative description of differences in telomeric fragment movement. In the case of angular flexibility this criterion is set to 10 degrees but for displacement flexibility is equal to 0.5 Å. Results of such analysis is presented in Figs. 4 and 5. The left columns in both figures present the averaged values of DNA parameters, while the right columns contain flexibility factors. Rows characterize three pairs belonging to canonical or modified XXX triad. From these figures it is possible to depict both the dynamic and structural features of central telomeric fragments.

The average structure of modified and canonical telomeric fragments are close each to other. Although, there are some trends in mean geometry alterations caused by the presence of 8-oxo-guanine, but they are usually smaller than the standard mean deviation. For example the structure C is characterized by lowest values of slide and twist parameters for all purines of central telomeric fragments among all studied DNA fragments. The difference is equal to 0.5 angstrom and 1.5 degrees, respectively. However, the standard mean deviation of tilt, roll, twist, buckle, propeller, and opening are in the range from 2.9 to 8.8. To the contrary the standard mean deviations of shear, stretch, stagger, shift, slide, and rise are all smaller than 0.6. The observation that there is only minor impact of the DNA oxidation on the average structure is consistent with previously reported molecular dynamic studies of DNA comprising 8-oxo-G:C base pair [17, 24, 25]. The structural differences between standard and modified central telomeric triad were quantitatively compared by means of deviation coefficient defined as follows:

$$\kappa = \sum_i |(\lambda_i^X - \lambda_i^A)/\lambda_i^A|$$

where  $\lambda_i$  denotes hydrogen bond length, angular or displacement parameters. Thus, values of this coefficient express the sum of absolute values of the relative deviations from A structure. Table 2 presents results of calculations of this deviation coefficient for each of purine belonging to central telomeric triad. Interestingly the most significant changes are observed for central 8-oxo-guanine. The greater the number of 8-oxo-G the more significant deviations from canonical structure. This suggests existence of the cumulative conformation alterations caused by the presence of several 8-oxo-G molecules.

Despite similarities in average structures the dynamic displacement properties are significantly affected by the presence of oxidized guanine. Usually flexibility with respect

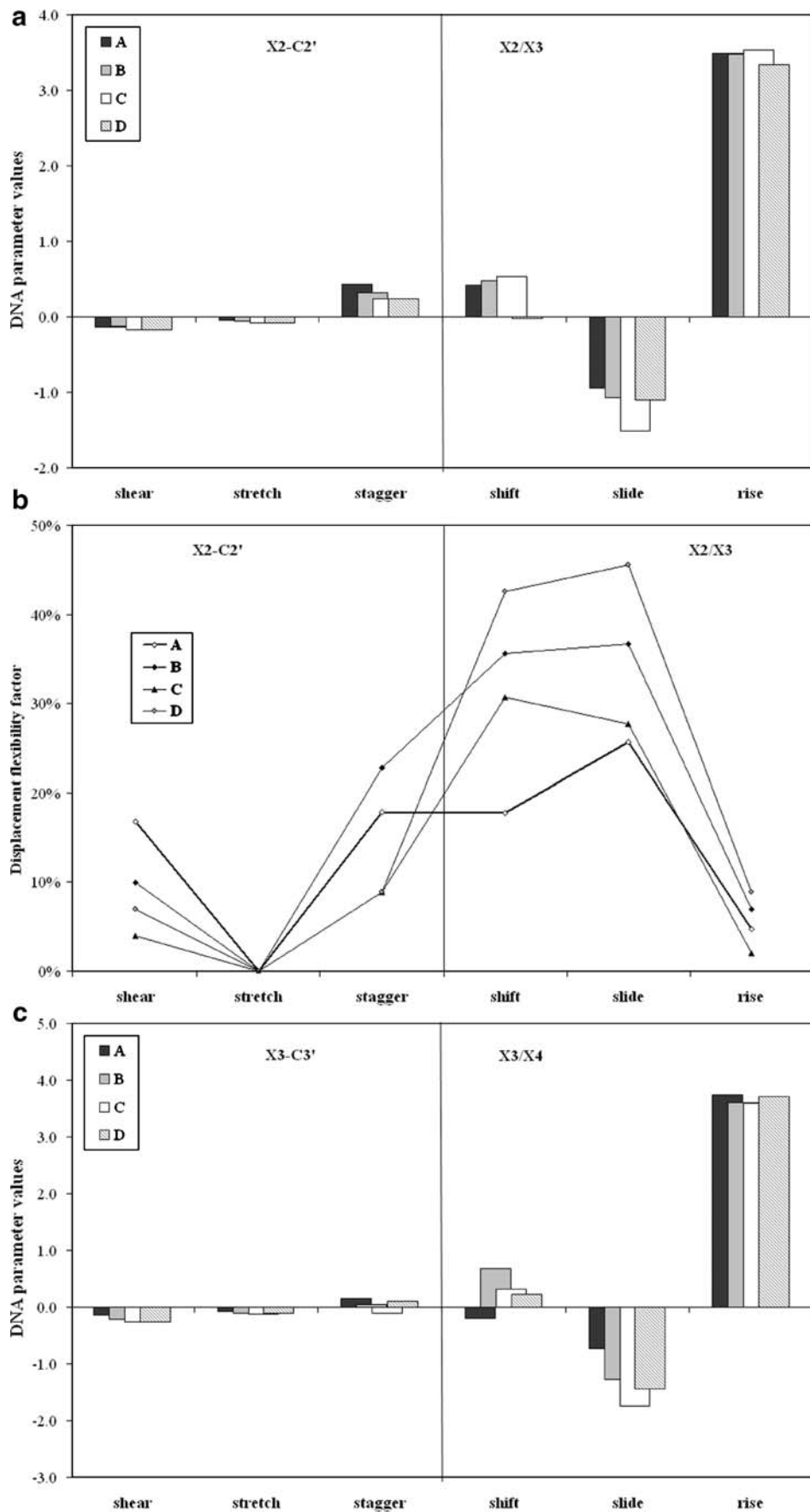
to parameters defining mutual orientation of base within the same strand are much higher than time variations of parameters declaring inter-strand mutual orientation of base pairs. The significant increase of mutual displacement of two successive base pairs along either axis of modified telomeric DNA compared to canonical one is especially visible for X<sub>2</sub>/X<sub>3</sub> and X<sub>4</sub>/T<sub>5</sub> pairs. For example the displacement flexibility factor of shift and slide for X<sub>2</sub>/X<sub>3</sub> of structures C and D is more than twice as high as for structure A. Besides, the movement of two successive base pairs along X axis of X<sub>4</sub>/T<sub>5</sub> pair of all modified central telomeric fragment is much higher than for structure A. For example almost 40% of time the shift parameter of X<sub>4</sub>/T<sub>5</sub> pair in oxidized structures is at least 10 degrees apart from the mean structure, but at the same time such variation for corresponding pair of structure A deviates from mean value only 20% of the time. This suggests that mutual displacement of two successive base pairs of all modified structures has higher amplitudes. Furthermore, the values of angular flexibility factors presented in Fig. 5 suggest that rotation of two successive pairs is less affected by oxidation of guanine than displacement flexibility factors. For all structures the successive pairs do not undergo opening. However, up to 20% of the time the propeller varies from the average structure by more than 10 degrees and the buckle may adopt values significantly changed with respect to the mean value more than 20% of time. The most significant change of this parameter is observed for X<sub>4</sub>-C<sub>4</sub> pair. In this case the structure A exhibits higher flexibility than oxidized telomeric fragment.

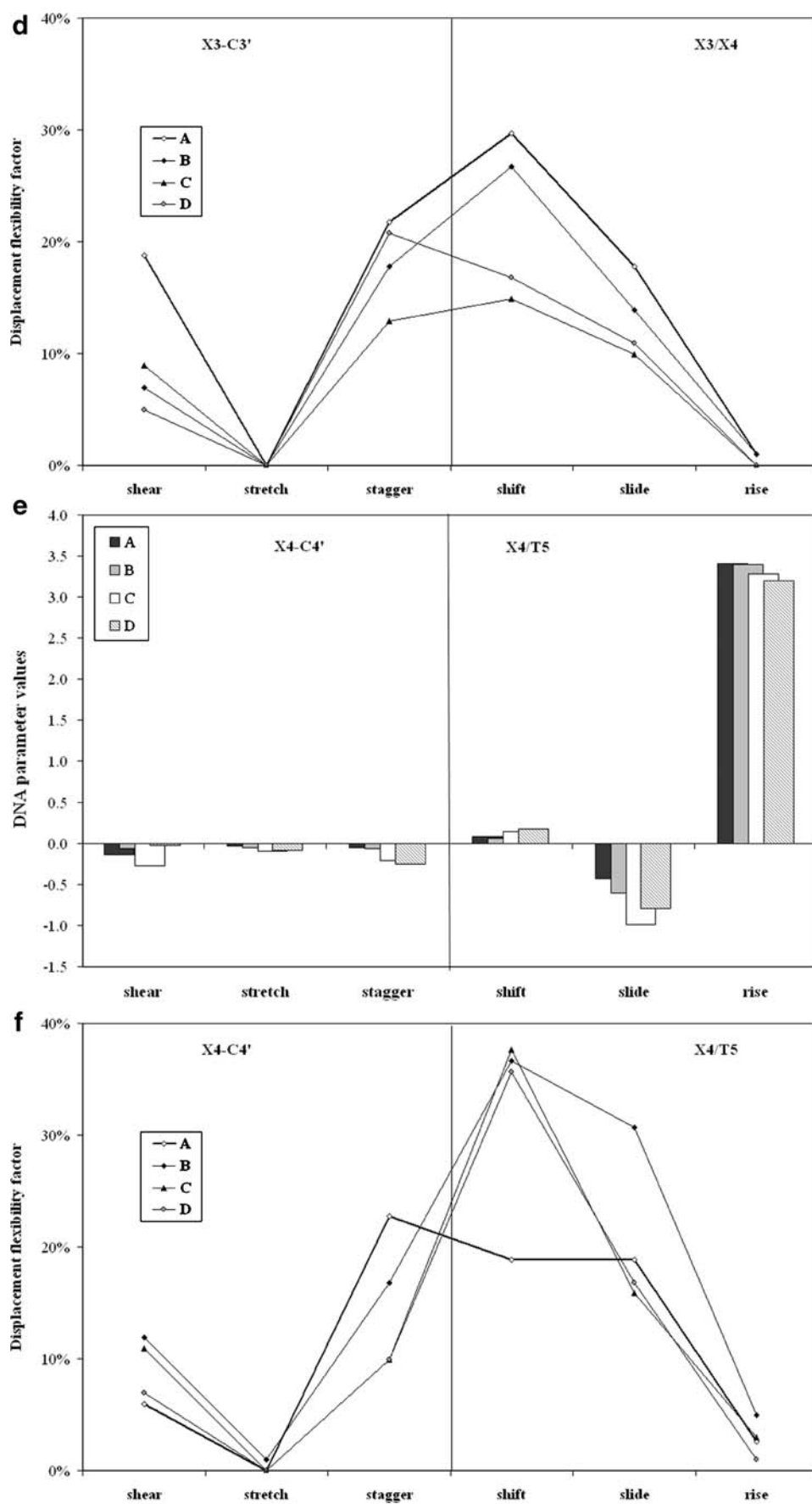
Thus, although there are observed only modest alterations of the mean values of oxidized and standard telomeric fragments the dynamic properties are significantly affected by presence of 8-oxo-guanine. The most significant changes are observed for shift flexibilities of the whole central triad and slide variation of the X<sub>2</sub> purine in the telomeric DNA. The presence of oxidized guanine increases amplitude of mutual displacement of two successive base pairs along X and Y axis. The only significant alteration of two bases rotation is observed about X axis for X<sub>4</sub>-C pair. This time, however, the stiffness of rotation is observed in case modified telomeric fragments.

#### Energetic consequences of guanine oxidation

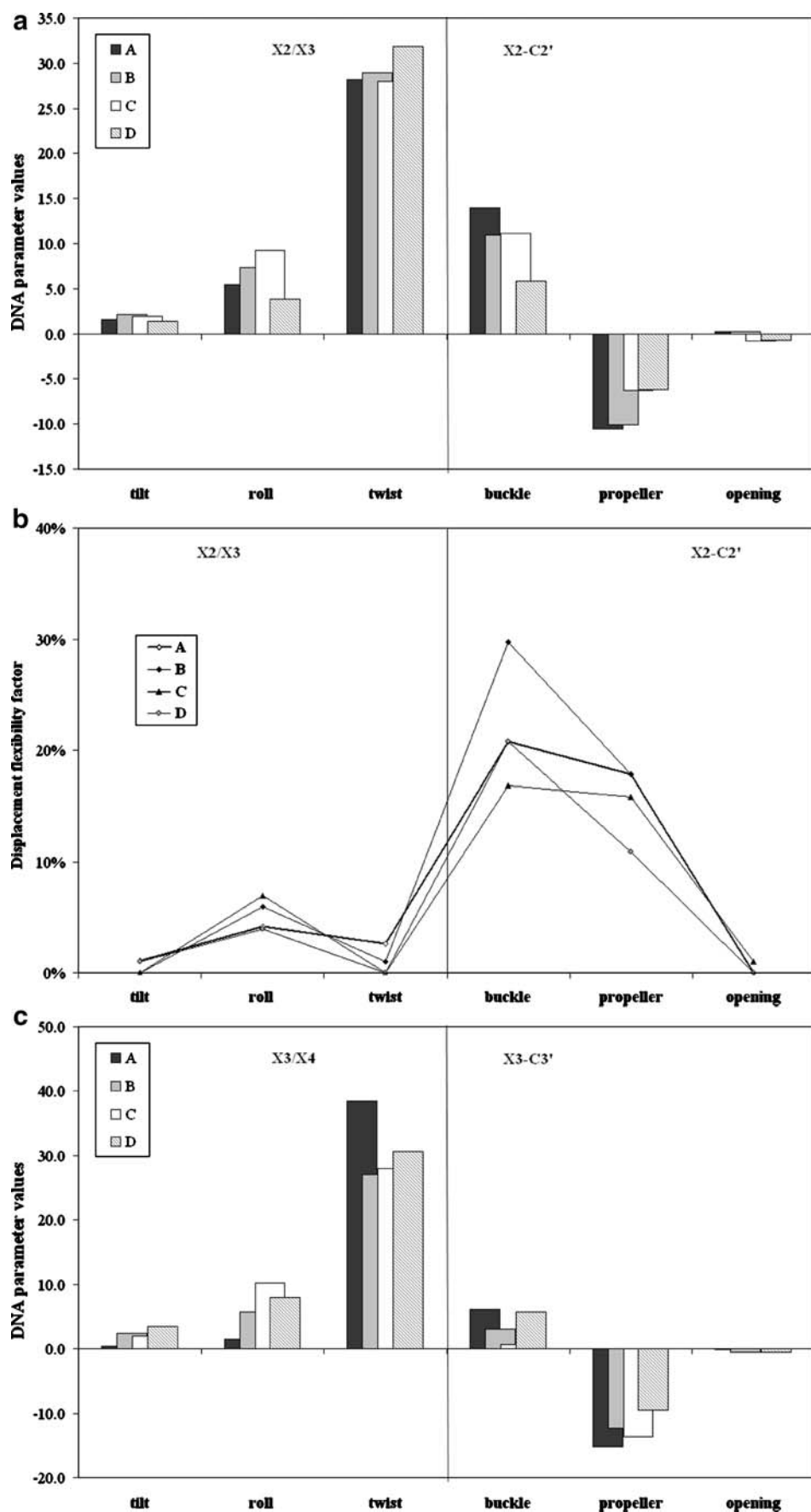
The energetic consequences of guanine oxidation in telomeric DNA fragments were characterized by energies of pair formation both of hydrogen bonded and stacked complexes. The counterpoise procedure was applied for correction of basis set superposition error [26, 27]. Results are presented in Table 3. According to previous observation [19] the correlation contribution to the energies of stacked complexes are of crucial importance. The stabilization occurs only after treating these complexes by post-SCF.

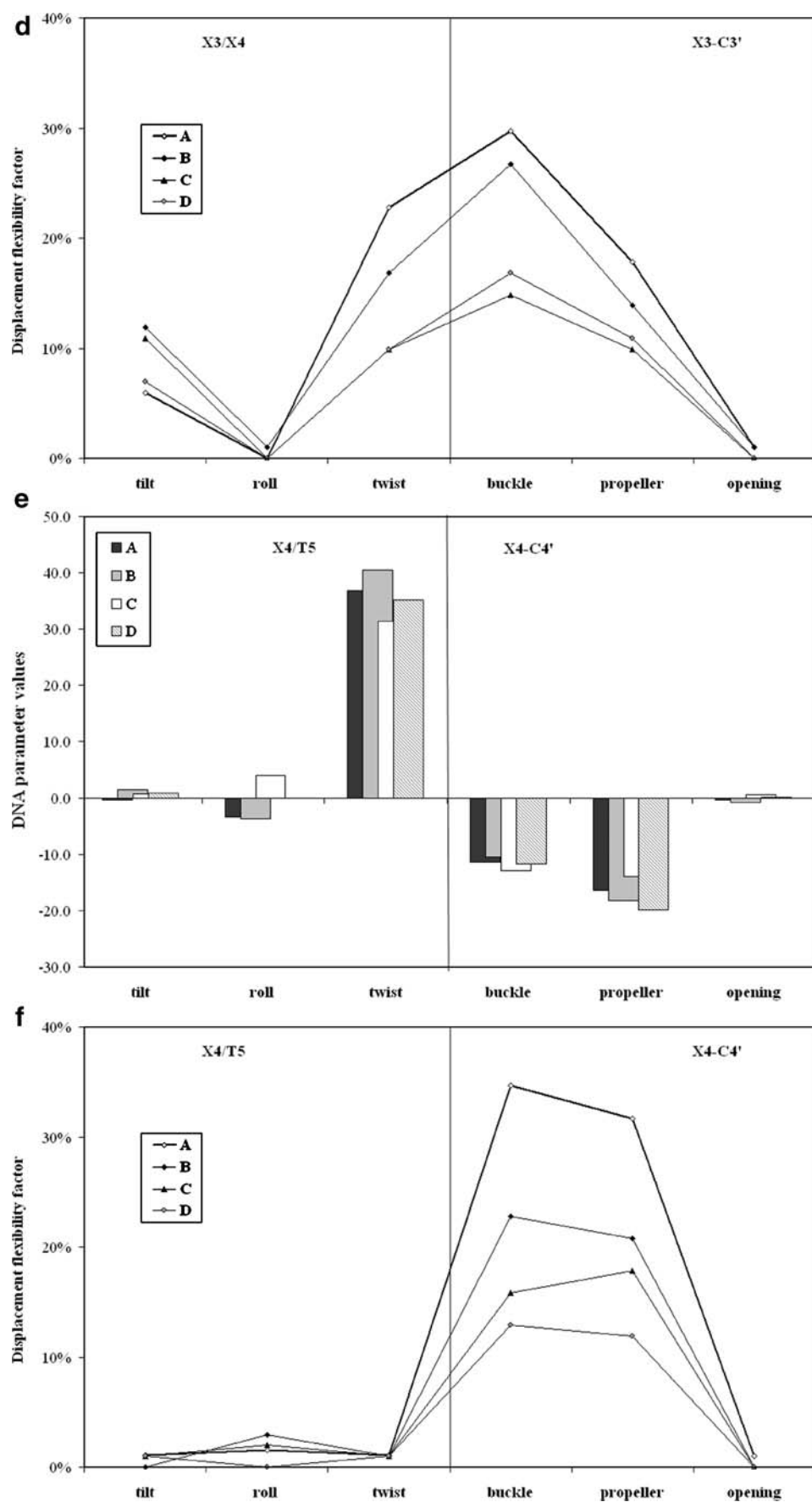
**Fig. 4** The averaged values of DNA parameters as well as their dynamics characteristics presented for central telomeric fragment of oligonucleotides defined in Table 1. The symbol X stands for guanine or 8-oxoguanine depending on oligomer type. The displacement flexibility factor is defined as a time percentage of adopting structures, for which the parameters values deviate from the mean value by more than 0.5 Å



**Fig. 4** (continued)

**Fig. 5** The averaged values of DNA parameters as well as their dynamics characteristics presented for central telomeric fragment of oligonucleotides defined in Table 1. The symbol X stands for guanine or 8-oxoguanine depending on oligomer type. The angular flexibility factor is defined as a time percentage of adopting structures, for which the parameters values deviate from the mean value by more than 10 degrees



**Fig. 5** (continued)

**Table 2** The values of deviation coefficient calculated for bases in central triad of oxidized telomeric fragments with respect to the canonical one

DNA	Base pair		
	X <sub>2</sub>	X <sub>3</sub>	X <sub>4</sub>
B	2.0	7.8	7.9
C	18.2	19.9	19.5
D	10.6	17.7	15.4

The energies of stacked complexes corresponding to mean A oligomer geometries are equal to  $-3.1$  and  $-3.5 \text{ kcal mol}^{-1}$  for  $5'\text{-G}_2/\text{G}_3\text{-3'}$  and  $5'\text{-G}_3/\text{G}_4\text{-3'}$ , respectively. The additional calculations for the whole GGG triad in its mean geometry was found to be equal to  $-7.5 \text{ kcal mol}^{-1}$ . This value has a meaning of trimer formation and half of this amount stands for average energy of G/G stacked dimer. Thus, the energy evaluated in separate calculations for stacked pairs is in qualitative agreement with results for trimer, what suggests that the stacked energies is fairly pair-wise additive in the studied oligomers. The replacement of guanine with 8-oxo-G at X<sub>3</sub> position results in almost a threefold increase of stabilization energies. This may be responsible for the observed increase of rigidity in case of oxidized telomeric fragments. Interestingly, there is significant context dependence on the stacking energy in case of B oligomer. The  $5'\text{-G}_2/8\text{-oxoG}_3\text{-3'}$  pair is almost twice as strongly bonded as  $5'\text{-8oxoG}_3/\text{G}_4\text{-3'}$  one. For C and D telomeric fragments the stacking energy is almost identical and equals about  $-7.3 \text{ kcal mol}^{-1}$ , what correspond to stacking of two modified guanine molecules. The energetics of hydrogen bonds formation may be quite satisfactory described on SCF level and taking into account the correlation effect reduces systematically the stabilization energies by amount about  $3 \text{ kcal mol}^{-1}$  the MP2/6-31G(d=0.25) energies were presented in Table 3. The strongest hydrogen complex with cytosine was formed by G<sub>3</sub> guanine in canonical telomeric fragment, while the weakest one among all studied here corresponds to 8oxoG<sub>3</sub> in D oligomer. However, the difference between energies of these two pairs is less than  $3 \text{ kcal mol}^{-1}$ . Thus, no significant impact of 8-oxo-guanine presence in telomeric fragments was found on hydrogen bonding with cytosine.

**Table 3** The energies (in  $\text{kcal mol}^{-1}$ ) of pair formation of both stacked and hydrogen bonded complexes in central telomeric triad of standard and oxidized oligomers

$\Delta E^{\text{MP2}}$		A	B	C	D
<b>stacking</b>	<b>X<sub>2</sub>/X<sub>3</sub></b>	-3.1	-8.7	-7.3	-7.3
	<b>X<sub>3</sub>/X<sub>4</sub></b>	-3.5	-4.8	-7.2	-7.5
<b>H-bonding</b>	<b>X<sub>2</sub>-C<sub>2</sub></b>	-23.6	-23.8	-22.9	-23.5
	<b>X<sub>3</sub>-C<sub>3</sub></b>	-24.5	-24.4	-23.5	-21.5
	<b>X<sub>4</sub>-C<sub>4</sub></b>	-23.1	-22.4	-22.2	-22.5

## Electrostatic consequences of presence of 8-oxo-guanine

The final aspects, which was studied in the context of differentiate of oxidized and canonical telomeres were the electrostatic and frontier orbitals properties. The TRF1 and TRF2 proteins interacting with DNA make contact with the edges of the base pairs that protrude into the major groove. In the case of purines the donor-acceptor interactions with the major groove of B-DNA are related to side groups at C<sub>6</sub> and N<sub>7</sub> centers along with oxygen atoms located on phosphate anion. Since 8-oxo-guanine is characterized by the bulk acceptor bounded to C<sub>8</sub> atom of imidazole ring and N<sub>7</sub> acceptor site is capped by the attached hydrogen atom it is reasonable to regard these circumstances as a major source of guanine recognition distortions. In Fig. 6 the isosurface contour plots were presented for MP2/6-31G(d=0.25) derived electrostatic potentials. As one may expect in the canonical form of telomeric DNA both G<sub>2</sub>/G<sub>3</sub> and G<sub>3</sub>/G<sub>4</sub> stacked pairs are characterized by almost identical electrostatic properties. To the contrary, the 8-oxo-guanine has quite different donor-acceptor pattern both for G<sub>2</sub>/8oxoG<sub>3</sub> and 8oxoG<sub>3</sub>/G<sub>4</sub> sequences. The N<sub>7</sub> group in native A telomere plays the role of acceptors site, while in oxidized oligonucleotides becomes the donor one. This is clearly visible on ESP plots. Besides, the electrostatic features of hydrogen-bonded complexes found in A and B DNA fragments are also presented in Fig. 5. The strong and uniform electronegative region present in native structure comes from O<sub>6</sub> oxygen and N<sub>7</sub> centers of guanine. In the case of 8-oxo-guanine the sources of electronegative vicinity is different. The O<sub>6</sub> along with O<sub>8</sub> oxygen atoms are responsible for this feature. However, due to the relatively long distance between these centers as well as the occurrence of donor at N<sub>7</sub> site separating the overlapping of the former two electronegative regions is impossible. Thus, the guanine pattern visible from the major groove may then be described as donor-acceptor-acceptor formed by H<sub>8</sub>-N<sub>7</sub>-O<sub>6</sub> atoms, respectively. To the contrary the presence of 8-oxo-guanine changes the electrostatic properties of the major groove into acceptor-donor-acceptor coming from O<sub>8</sub>-H<sub>7</sub>-O<sub>6</sub> atoms.

Furthermore, the frontier orbital properties are also significantly affected by guanine oxidation as presented in Fig. 7. Interestingly the distribution of HOMO is not uniform in the case of A oligomer. Most densities of this orbital is placed on G<sub>2</sub> and G<sub>3</sub>. To the contrary LUMO is predominantly located on the last guanine molecule in the analyzed triad. This suggests that different guanine molecules will be responsible for electro-donating end electro-accepting properties. The presence of 8-oxo-guanine in the analyzed triad completely change the dislocation of frontier orbitals. Almost 90% of the HOMO is located on G<sub>4</sub> guanine, while both G<sub>2</sub> and 8-oxo-G<sub>3</sub> have only minor contribution to

**Fig. 6** The 0.05 isosurface contours of MP2/6-31G( $d=0.25$ ) derived electrostatic potential are drawn for chosen pairs of A and B oligomers. The symbol X stands for guanine or 8-oxo-guanine

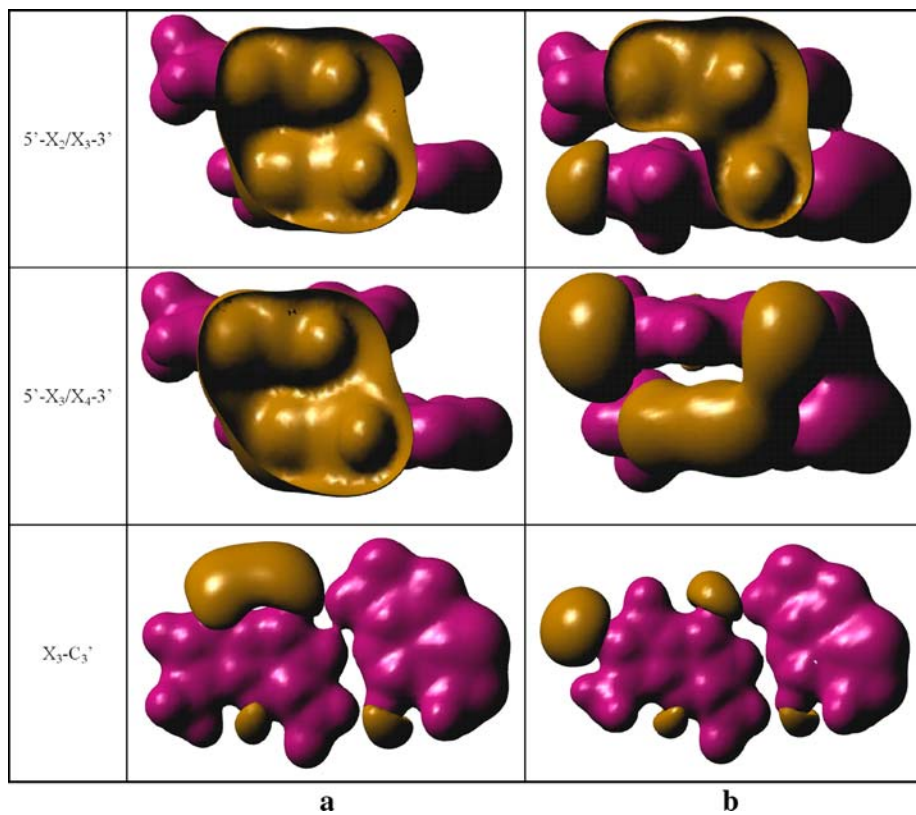
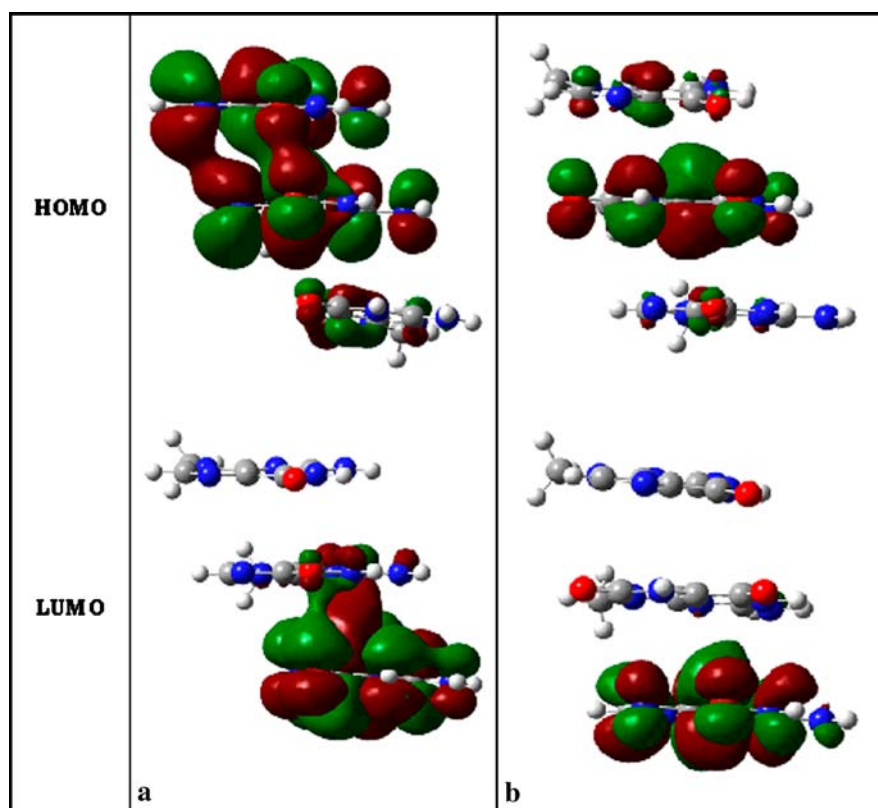


**Fig. 7** The frontier orbital distribution in canonical and oxidized central triad of telomeric B-DNA fragments. The isodensity contour correspond to 0.01 value of molecular orbital densities



this orbital. The electro-accepting properties of canonical and modified telomeric fragments are similar since most of LUMO is localized on G<sub>4</sub>. It is noteworthy that although 8-oxo-G has greater electron affinity than guanine itself and LUMO should be localized to oxidized guanine rather than to native one the location of this frontier orbital is context dependent. Similarly, the 8-oxo-G is less susceptible to oxidation than guanine and one may expect localization of HOMO to the one of guanines rather than to 8-oxo-G. However context dependence also take place in this case. For 5'-G<sub>1</sub>/X<sub>2</sub>-3' sequence HOMO is located on guanine and LUMO on 8-oxo-G, while in case of 5'-X<sub>2</sub>/G<sub>3</sub>-3' sequence the frontier orbitals are reversed. Thus, both electrostatic and molecular orbital properties are significantly affected by oxidation of telomeric B-DNA fragments.

## Conclusions

The results presented above of the molecular dynamics simulations supplemented with *ab initio* calculations revealed intricate consequences of DNA telomeric fragment oxidation. The central triad containing 8-oxo-guanine in the place of guanine significantly changes its dynamic properties, energetic characteristics as well as electrostatic and frontier orbital features. This in turn will result in different binding abilities of such damaged telomeric fragments. Although results presented in this study give only the qualitative insight into the observed difference in binding of proteins to canonical and oxidized telomeric DNA, the potential sources of observed alteration in binding percentage are pointed out. The structural and dynamic behavior of modified telomeric fragments, the quantitative analysis of pair-wise contribution of amino acid-nucleic acid to energetic and entropic terms of protein-DNA affinity, the susceptibility of telomeric to the oxidized medium are only a few open questions of especial importance. Since telomerase is absent in most normal tissues and approximately 87% of all primary human cancers [28] express telomerase activity enabling tumor cells to maintain telomere length and indefinite replicative capacity further investigations are worthy. These problems will be addressed in further investigations.

**Acknowledgements** Results were obtained based on computational grants from PCSS (Poznań Supercomputing and Networking Centre, Poland). The allocation of computing time is greatly appreciated.

## References

- Fairall L, Chapman L, Moss H, de Lange T, Rhodes D (2001) Mol Cell 8:351–361
- Lundblad V (2000) Mutat Res 451:227–240
- De Lange T (2002) Oncogene 21:532–540
- Chong L, van Steensel B, Broccoli D, Erdjument-Bromage H, Hanish J, Tempst P, de Lange T (1995) Science 270:1663–1667
- Broccoli D, Smogorzewska A, Chong L, de Lange T (1997) Nat Genet 17:231–235
- Harley CB, Futcher AB, Greider CW (1990) Nature 345:458–460
- von Zglinicki T, Serra V, Lorenz M, Saretzki G, Lenzen-Grossmlighaus R, Gressner R, Risch Steinhagen-Thiessen E (2000) Lab Invest 80:1739–1747
- Bodnar AG, Ouellette M, Frolkis M, Holt SE, Chiu CP, Morin GB, Harley CB, Shay JW, Lichtsteiner S, Wright WE (1998) Science 279:349–352
- Tchirkov A, Lansdorp PM (2003) Hum Mol Genet 12:227–232
- von Zglinicki T (2002) Trends Biochem Sci 27:339–344
- Saretzki G, von Zglinicki T (2002) Ann NY Acad Sci 959: 24–29
- Opresko PL, Fan J, Danzyl S, David M, Wilson DM III, Bohr VA (2005) Nucleic Acids Res 33:1230–1239
- Cysewski P (2005) Z Phys Chem 219:213–234
- Court R, Chapman L, Fairall L, Rhodes D (2005) EMBO Rep 6:39–45
- Hanaoka S, Nagadoi A, Nishimura Y (2005) Protein Sci 14:119–130
- Lu XJ, Olson WK (2003) Nucleic Acids Res 31:5108–5121
- Miller JH, Fan-Chiang ChP, Straatsma TP, Kennedy MA (2003) J Am Chem Soc 125:6331–6336
- Case DA, Darden TA, Cheatham TE III, Simmerling CL, Wang J, Duke RE, Luo R, Merz KM, Wang B, Pearlman DA, Crowley M, Brozell S, Tsui V, Gohlke H, Mongan J, Hornak V, Cui G, Beroza P, Schafmeister C, Caldwell JW, Ross WS, Kollman PA (2004) AMBER 8. University of California, San Francisco
- Cysewski P, Czyżnikowska-Balcerak Ź (2005) J Mol Struct (THEOCHEM) 757:29–36
- Cysewski P, Czyżnikowska-Balcerak Ź, Szefler B (2003) Pol J Chem 77:287–1300
- Frisch MJ, Trucks GW, Schlegel HB, Scuseria GE, Robb MA, Cheeseman JR, Montgomery JA Jr, Vreven T, Kudin KN, Burant JC, Millam JM, Iyengar SS, Tomasi J, Barone V, Mennucci B, Cossi M, Scalmani G, Rega N, Petersson GA, Nakatsuji H, Hada M, Ehara M, Toyota K, Fukuda R, Hasegawa J, Ishida M, Nakajima T, Honda Y, Kitao O, Nakai H, Klene M, Li X, Knox JE, Hratchian HP, Cross JB, Bakken V, Adamo C, Jaramillo J, Gomperts R, Stratmann RE, Yazyev O, Austin AJ, Cammi R, Pomelli C, Ochterski JW, Ayala PY, Morokuma K, Voth GA, Salvador P, Dannenberg JJ, Zakrzewski VG, Dapprich S, Daniels AD, Strain MC, Farkas O, Malick DK, Rabuck AD, Raghavachari K, Foresman JB, Ortiz JV, Cui Q, Baboul AG, Clifford S, Cioslowski J, Stefanov BB, Liu G, Liashenko A, Piskorz P, Komaromi I, Martin RL, Fox DJ, Keith T, Al-Laham MA, Peng CY, Nanayakkara A, Challacombe M, Gill PMW, Johnson B, Chen W, Wong MW, Gonzalez C, Pople JA (2004) Gaussian 03, Revision C.02, Gaussian, Inc, Wallingford CT
- Dennington R II, Keith T, Millam J, Eppinnett K, Hovell W Lee, and Gilliland R (2003) GaussView, Version 3.09 Semichem, Inc, Shawnee Mission, KS
- Dickerson RE, Bansal M, Calladine CR, Diekmann S, Hunter WN, Kennard O, Laverty R, Nelson HCM, Olson WK, Saenger W, Shakked Z, Sklenar H, Soumpasis DM, Tung ChS, Wang AHJ, Zhurkin VB (1989) Nucleic Acids Res 17:1797–1803
- Dodson ML, Lloyd RS (2001) Mutat Res 487:93–108
- Ishida H (2002) J Biomol Struct Dyn 19:839–851
- Simon S, Duran M, Dannenberg JJ (1996) J Chem Phys 105:11024–11031
- Boys SF, Bernardi F (1970) Mol Phys 19:553
- Lichtsteiner SP, Lebkowski JS, Vasserot AP (1999) Ann NY Acad Sci 886:1–11